Acta Cryst. (1976). B32, 2427

Unique Face-Sharing Octahedral Chains in Ferrous Chlorophosphate, $Fe_2(PO_4)Cl$

BY J. B. ANDERSON, J. R. REA AND E. KOSTINER

Institute of Materials Science and Department of Chemistry, University of Connecticut, Storrs, Connecticut 06268, *U.S.A.*

(*Received* 17 *February* 1976; *accepted* 26 *March* 1976)

Ferrous chlorophosphate, $Fe_2(PO_4)Cl$, crystallizes in the space group $C2/c$, with unit-cell dimensions $a=13{\cdot}677$ (1), $b=9{\cdot}217$ (1), $c=9{\cdot}326$ (1) Å, and $\beta=132{\cdot}53$ (1)° ($Z=8$). A three-dimensional structural analysis, using automatic-diffractometer data, has been completed and refined by full-matrix least-squares procedures to a residual $R=0{\cdot}047$ ($R_w=0{\cdot}089$). The unique and unusual structure contains chains of face-sharing iron-containing octahedra; each of the three crystallographically unique iron atoms is coordinated by four oxygens and by two chlorines in *trans* positions. The Fe(1) polyhedron shares *adjacent* faces with Fe(2) and Fe(3) polyhedra in a grouping similar to that found in the mineral seamanite. Each Fe(2) and Fe(3) polyhedron shares opposite faces with Fe(1) polyhedra, resulting in infinite chains of face-sharing polyhedra. Mössbauer-effect and magnetic-susceptibility measurements confirm the presence of divalent iron and indicate antiferromagnetic ordering at a temperature below 9K [$\theta=-29$ (2)K].

Introduction

As a part of our continuing study of the crystal chemistry of compounds having the stoichiometry $M_2(PO_4)Z$, where M is a divalent metal ion and Z is a halogen, single crystals of ferrous chlorophosphate, $Fe_2(PO_4)Cl$, have been prepared, and a complete structural analysis by X-ray diffraction has been carried out. The compound crystallizes in the space group $C2/c$ and has a unique and very unusual structure characterized by infinite chains of face-sharing iron-containing octahedra. Some segments of the chains are similar to the linear face-sharing trimers found in several basic iron phosphates (Moore, 1970), and other segments are similar to the most unusual adjacent-face-sharing trimers found in seamanite (Moore, 1971).

Mössbauer-effect and magnetic-susceptibility measurements were also carried out for the compound. The Mössbauer effect data confirm the presence of iron in oxidation state II exclusively. The magnetic data indicate antiferromagnetic ordering at a temperature below 9 K.

Experimental

Crystals of $Fe_2(PO_4)Cl$ were grown by standard flux techniques from an excess of $FeCl_2$. A mixture of $Fe_3(PO_4)_2$ (Kostiner & Rea, 1974) and $FeCl_2$ in a mole ratio of 40:60 was packed into a 5 mm diameter gold tube which had been welded closed at one end. The tube was loosely crimped at the other end and sealed under vacuum in a vitreous silica tube to prevent oxidation of the ferrous ion. After heating for several hours at 950 °C the charge was cooled at 16 °C h^{-1} to 300 ° and then removed from the furnace. Pale orange crystals of $Fe_2(PO_4)Cl$ were mechanically separated from the mixture.

Iron-57 Mössbauere-ffect spectra were recorded with a Nuclear Science and Engineering Corporation Model NS-1 spectrometer operating in the constant acceleration mode. The data were collected with a multichannel analyzer using a 20 mCi ^{57}Co/Pd source. Magnetic susceptibility measurements were made on a PAR Model 155 vibrating sample magnetometer with related cryogenic accessories.

An irregularly shaped crystal having maximum and minimum dimensions of 0·28 and 0·11 mm, respectively, was selected for X-ray diffraction analysis. Precession photographs revealed monoclinic symmetry with systematic absences corresponding to space groups $C2/c$ or Cc. Subsequent analysis showed the space group to be $C2/c$ (see below), and the final refinements were carried out in this space group.

The lattice parameters were determined in a *PICK*-II least-squares refinement program, using 48 reflections within the angular range $32°<2\theta<51°$; the reflections were automatically centered on a Picker FACS-I four-circle diffractometer using Mo $K\alpha_1$ radiation ($\lambda=0{\cdot}70930$ Å). At 22 °C the lattice parameters are $a=13{\cdot}677$ (1), $b=9{\cdot}217$ (1), $c=9{\cdot}326$ (1) Å, and $\beta=132{\cdot}53$ (1)°, where the figures in parentheses represent the standard deviations in the last reported figure. The calculated density, with $Z=8$, is 3·712 g cm^{-3}. It should be noted here that any one of four *C*-centered unit cells having β in the close range between 132·5 and 137·0° could have been chosen. Following the Donnay convention, we chose the *C*-centered cell having β closest to 90°, giving the shortest cell edges. (The *I*-centered cell having the shortest cell edges had $\beta=90{\cdot}44°$.)

Diffraction intensities were measured using Zr-filtered Mo $K\alpha$ radiation at a take-off angle of 2·5° with the diffractometer operating in the θ–2θ scan mode. Scans were made at 1° min^{-1} over 1·0° with allowance for dispersion and with 20 s background counts taken at both ends of the scan. Of the 1998 independent data investigated in the angular range $2\theta<71°$, 1964 were

considered observable according to the criterion $|F_o| > 5{\cdot}0\sigma_F$, where σ_F is defined as $0{\cdot}02|F_o|+(C+k^2B)^{1/2}/2|F_o|\mathrm{Lp}$; the total scan count is C, k is the ratio of scanning time to the total background time, and B is the total background count. Three reflections were systematically monitored; the maximum variation in intensity observed was never greater than $\pm 2\%$ over the data collection period.

Intensity data were corrected for Lorentz and polarization effects, and absorption corrections ($\mu = 77{\cdot}2$ cm^{-1}, Mo $K\alpha$) were made with a computer program written by N. W. Alcock and B. Lee for a crystal of general shape. Input for the program included the indices of the plane faces of the crystal, which were determined with the aid of precession photographs, and the orientation angles of the crystal coordinate system with respect to the diffractometer coordinate system, which were obtained from the program *PICK*-II.

The unit-cell volume of the crystal under study was almost identical with that of $Mn_2(PO_4)Cl$ (Rea & Kostiner, 1972*a*) after a correction factor based on the relative radii of Mn^{2+} and Fe^{2+} was applied. Hence, to resolve the structure, the unit-cell contents $Fe_{16}(PO_4)_8Cl_8$ in space group $C2/c$ were used in the multisolution symbolic addition program *MULTAN* (Germain, Main & Woolfson, 1971). Phases with a probability of being greater than 75% correct were used in the starting set. The strongest peaks in the best electron density map generated by *MULTAN* from these reflections proved to be due to Fe and P atoms. Difference Fourier maps revealed the locations of the Cl and O atoms. A similar analysis assuming the space group Cc was carried out with the result that all the atoms appeared in the same positions as previously; therefore, space group $C2/c$ was used in the refinement.

Because of the unusual features of the structure an independent analysis was made of the Patterson map, by standard techniques. Again the same heavy-atom positions were found.

Full-matrix least-squares refinement (Busing, Martin & Levy, 1962) using a $1/\sigma^2$ weighting scheme, zerovalent scattering factors for Fe, P, Cl and O (*International Tables for X-ray Crystallography*, 1974), isotropic temperature factors, and correction for secondary extinction and anomalous dispersion, yielded a residual $R = 0{\cdot}067$ and a weighted residual $R_w = 0{\cdot}106$. Anisotropic refinements in which the occupancies of the Fe and Cl sites were allowed to vary indicated full occupancies. Therefore, all occupancies were fixed at 100% for subsequent refinements. The final anisotropic refinement, based on a data:parameter ratio of 27 with 74 independently varied parameters, yielded $R = 0{\cdot}047$ and $R_w = 0{\cdot}089$ for the observed

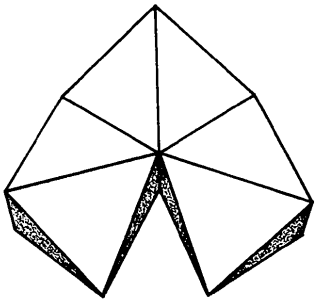

Fig. 1. Illustration of one type of adjacent-face-sharing for regular octahedra. The two lower free vertices are sterically hindered for regular O octahedra.

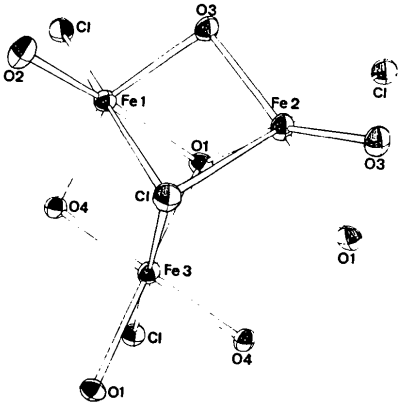

Fig. 2. The structural unit of $Fe_2(PO_4)Cl$ corresponding to Fig. 1. The distorted octahedron with Fe(1) at the center shares adjacent faces with octahedra containing Fe(2) and Fe(3) respectively. The two free vertices at O(1) and O(4) are bridged by a P atom. For clarity the orientation shown is different from that of Fig. 1.

Table 1. *Fractional atomic coordinates* ($\times 10^4$) *and anisotropic thermal parameters*

Numbers in parentheses are estimated standard deviations in the last significant figure. The B's are defined by the general temperature factor $\exp[-\frac{1}{4}(B_{11}h^2a^{*2}+B_{22}k^2b^{*2}+B_{33}l^2c^{*2}+2B_{12}hka^*b^*+2B_{13}hla^*c^*+2B_{23}klb^*c^*)]$.

	x	y	z	B_{11}	B_{22}	B_{33}	B_{12}	B_{13}	B_{23}
Fe(1)	3122·4 (5)	2415·0 (6)	3235·1 (8)	0·60 (2)	0·76 (2)	0·62 (2)	−0·10 (1)	0·39 (2)	−0·06 (1)
Fe(2)	5000	2169·5 (9)	2500	0·45 (3)	1·31 (3)	0·54 (3)	0	0·28 (2)	0
Fe(3)	0	0	0	0·56 (3)	0·93 (3)	0·75 (3)	0	0·42 (2)	0
P	2699·7 (9)	4892 (1)	178 (1)	0·43 (3)	0·65 (3)	0·43 (3)	−0·06 (2)	0·26 (3)	−0·04 (2)
O(1)	3724 (3)	3999 (3)	2104 (4)	0·63 (8)	1·00 (8)	0·42 (8)	−0·08 (7)	0·25 (7)	−0·04 (6)
O(2)	3017 (3)	958 (3)	4607 (5)	0·98 (9)	1·38 (10)	1·17 (10)	−0·11 (8)	0·75 (9)	0·22 (8)
O(3)	3294 (3)	1149 (3)	1512 (4)	0·46 (8)	1·12 (8)	0·63 (8)	−0·15 (6)	0·30 (7)	−0·11 (7)
O(4)	3504 (3)	4349 (3)	4780 (4)	0·55 (8)	0·80 (8)	0·89 (9)	−0·03 (6)	0·50 (7)	−0·16 (7)
Cl	702·9 (9)	2727 (1)	752 (1)	0·58 (3)	1·19 (3)	0·64 (3)	−0·04 (3)	0·30 (3)	−0·06 (2)

data.* The maximum extinction correction (Zachariasen, 1968) was 15% of $|F_o|$ for the $\bar{4}04$ reflection. Table 1 lists the final positional and anisotropic thermal parameters.

Discussion

There are three Fe atoms in the asymmetric unit. Fe(1) is on a general position; Fe(2) is on a twofold axis; and Fe(3) is on an inversion center. Each iron is coordinated by four O and by two Cl atoms in *trans* positions. Table 2 lists the angles and distances for these distorted octahedra. The standard deviations for all bond lengths and bond angles were computed by the function and error program (*ORFFE*) of Busing Martin & Levy (1964).

The phosphate tetrahedron is quite distorted (Table 3). The average P–O distance is 1·536 Å (+0·034, −0·043 Å) and the average angle is 109·5° (+2·4, −3·1°).

The large variation in Fe–O distances and the distortions in the phosphate tetrahedron may be attributed in large part to the imbalance in the coordination about the O atoms in the structure. O(3) and O(4) are each bonded to two Fe and the P atom, but O(1) is bonded to three Fe and the P atom and O(2) is

* A list of structure factors has been deposited with the British Library Lending Division as Supplementary Publication No. SUP 31768 (11 pp., 1 microfiche). Copies may be obtained through The Executive Secretary, International Union of Crystallography, 13 White Friars, Chester CH1 1 NZ, England.

Table 3. *Bond distances, polyhedral edge lengths, and bond angles for the phosphate tetrahedron*

Numbers in parentheses are estimated standard deviations in the last significant figure.

(i) Interatomic distances (Å)			
P–O(1)	1·570 (3)	O(1)–O(2)	2·518 (5)
P–O(2)	1·493 (3)	O(1)–O(3)	2·535 (4)
P–O(3)	1·535 (3)	O(1)–O(4)	2·494 (4)
P–O(4)	1·545 (3)	O(2)–O(3)	2·482 (4)
		O(2)–O(4)	2·517 (4)
		O(3)–O(4)	2·498 (4)
(ii) Angles (°)			
O(1)–P–O(2)	110·6 (2)	O(2)–P–O(3)	110·1 (2)
O(1)–P–O(3)	109·5 (2)	O(2)–P–O(4)	111·9 (2)
O(1)–P–O(4)	106·4 (2)	O(3)–P–O(4)	108·4 (2)

Table 2. *Bond distances, polyhedral edge lengths, and bond angles for iron polyhedra*

Numbers in parentheses are estimated standard deviations in the last significant figure.

Fe(1) octahedron		Fe(2) octahedron			Fe(3) octahedron		
(i) Interatomic distances (Å)							
Fe(1)–O(1)	2·257 (3)	Fe(2)–O(1)	2×	2·270 (3)	Fe(3)–O(1)	2×	2·196 (3)
Fe(1)–O(2)	1·927 (3)	Fe(2)–O(3)	2×	2·067 (3)	Fe(3)–O(4)	2×	2·006 (3)
Fe(1)–O(3)	2·123 (3)	Fe(2)–Cl	2×	2·488 (1)	Fe(3)–Cl	2×	2·612 (1)
Fe(1)–O(4)	2·144 (3)						
Fe(1)–Cl	2·457 (1)						
Fe(1)–Cl′	2·604 (1)						
O(1)–O(3)	2·666 (4)	O(1)–O(1′)		3·040 (6)	O(1)–O(4)	2×	2·729 (4)
O(1)–O(4)	2·729 (4)	O(1)–O(3)	2×	2·666 (4)	O(1)–Cl	2×	3·782 (3)
O(1)–Cl	3·605 (3)	O(1)–Cl	2×	3·614 (3)	O(1)–Cl′	2×	2·997 (3)
O(1)–Cl′	2·997 (3)	O(1)–Cl′	2×	2·997 (3)	O(1′)–O(4)	2×	3·201 (4)
O(2)–O(3)	3·160 (4)	O(3)–O(3′)		3·681 (5)	O(4)–Cl	2×	3·442 (3)
O(2)–O(4)	3·177 (4)	O(3)–Cl	2×	3·367 (3)	O(4)–Cl′	2×	3·138 (3)
O(2)–Cl	3·197 (3)	O(3)–Cl′	2×	3·154 (3)			
O(2)–Cl′	3·287 (3)						
O(3)–Cl	3·432 (3)						
O(3)–Cl′	3·154 (3)						
O(4)–Cl	3·401 (3)						
O(4)–Cl′	3·138 (3)						
(ii) Angles (°)							
O(1)–Fe(1)–O(3)	74·9 (1)	O(1)–Fe(2)–O(1′)		84·1 (1)	O(1)–Fe(3)–O(4)	2×	80·9 (1)
O(1)–Fe(1)–O(4)	77·0 (1)	O(1)–Fe(2)–O(3)	2×	75·7 (1)	O(1)–Fe(3)–Cl	2×	103·4 (1)
O(1)–Fe(1)–Cl	99·7 (1)	O(1)–Fe(2)–Cl	2×	98·7 (1)	O(1)–Fe(3)–Cl′	2×	76·6 (1)
O(1)–Fe(1)–Cl′	75·7 (1)	O(1)–Fe(2)–Cl′	2×	77·9 (1)	O(1′)–Fe(3)–O(4)	2×	99·1 (1)
O(2)–Fe(1)–O(3)	102·5 (1)	O(3)–Fe(2)–O(3′)		125·9 (2)	O(4)–Fe(3)–Cl	2×	95·5 (1)
O(2)–Fe(1)–O(4)	103·2 (1)	O(3)–Fe(2)–Cl	2×	94·9 (1)	O(4)–Fe(3)–Cl′	2×	84·5 (1)
O(2)–Fe(1)–Cl	92·9 (1)	O(3)–Fe(2)–Cl′	2×	87·1 (1)			
O(2)–Fe(1)–Cl′	91·8 (1)						
O(3)–Fe(1)–Cl	96·8 (1)	O(1′)Fe(2)–O(3)	2×	157·3 (1)			
O(3)–Fe(1)–Cl′	83·0 (1)	Cl—Fe(2)–Cl′		175·6 (1)			
O(4)–Fe(1)–Cl	95·6 (1)						
O(4)–Fe(1)–Cl′	82·5 (1)						
O(1)–Fe(1)–O(2)	167·4 (1)						
O(3)–Fe(1)–O(4)	150·8 (1)						
Cl—Fe(1)–Cl′	175·3 (1)						

bonded only to one Fe and the P atom. This imbalance is compensated for by the fact that the bonds to O(1) are longer than average, whereas the bonds to O(2) are shorter than average. The average of all Fe–O bonds in the structure is 2·126 Å. The average O(3)–Fe and O(4)–Fe bonds are, respectively, 2·095 and 2·065 Å; O(1)–Fe is 2·241 and O(2)–Fe is 1·927 Å. Similarly, O(1)–P at 1·570 Å is much longer than the average P–O distance (1·536 Å), and O(2)–P at 1·493 Å is much shorter. The coordination about the anions is summarized in Table 4.

Table 4. *Bond distances* (Å) *and bond angles* (°) *for the anion polyhedra*

(i) Cl polyhedron			
Cl–Fe(1)	2·457 (1)	Fe(1)–Cl–Fe(2)	108·5 (4)
Cl–Fe(2)	2·488 (1)	Fe(1)–Cl–Fe(1)	170·0 (7)
Cl–Fe(1)	2·604 (1)	Fe(1)–Cl–Fe(3)	99·1 (4)
Cl–Fe(3)	2·612 (1)	Fe(2)–Cl–Fe(1)	74·4 (3)
		Fe(2)–Cl–Fe(3)	86·6 (3)
		Fe(3)–Cl–Fe(3)	71·4 (3)
(ii) O(1) polyhedron			
O(1)–P	1·570 (3)	P——O(1)–Fe(3)	122·6 (2)
O(1)–Fe(3)	2·196 (3)	P——O(1)–Fe(1)	123·3 (2)
O(1)–Fe(1)	2·257 (3)	P——O(1)–Fe(2)	124·7 (2)
O(1)–Fe(2)	2·270 (3)	Fe(3)–O(1)–Fe(1)	86·2 (1)
		Fe(3)–O(1)–Fe(2)	103·2 (1)
		Fe(1)–O(1)–Fe(2)	85·8 (1)
(iii) O(2) polyhedron			
O(2)–P	1·493 (3)	P–O(2)–Fe(1)	153·9 (2)
O(2)–Fe(1)	1·927 (3)		
(iv) O(3) polyhedron			
O(3)–P	1·535 (3)	P——O(3)–Fe(2)	133·7 (2)
O(3)–Fe(2)	2·067 (3)	P——O(3)–Fe(1)	130·3 (2)
O(3)–Fe(1)	2·123 (3)	Fe(2)–O(3)–Fe(1)	94·7 (1)
(v) O(4) polyhedron			
O(4)–P	1·545 (3)	P——O(4)–Fe(3)	133·1 (2)
O(4)–Fe(3)	2·006 (3)	P——O(4)–Fe(1)	130·9 (2)
O(4)–Fe(1)	2·124 (3)	Fe(3)–O(4)–Fe(1)	94·9 (1)

The most striking feature of the structure is that each Fe(1) polyhedron shares one face with an Fe(3) polyhedron and shares an *adjacent* face with an Fe(2) polyhedron. The Fe(2) and Fe(3) polyhedra thus share edges. This trimer, heretofore observed only in seamanite (Moore, 1971), is shown for regular octahedra in Fig. 1 and for the present structure in Fig. 2, which for clarity is viewed from a different perspective from Fig. 1. As pointed out by Moore (1971), the two free vertices on the lower part of Fig. 1 are prohibitively close (1·5 Å) for regular O octahedra with edges of 3·0 Å. However, in seamanite the O atoms at the two vertices are bridged by a boron-containing tetrahedron, which stabilizes the O atoms at a distance of 2·35 Å. In $Fe_2(PO_4)Cl$ the trimer is not as sterically hindered because the presence of the Cl ion shared by the three Fe enlarges the dihedral angle between the two free vertices. There is further stabilization by a phosphate bridge across O(1) and O(4) similar to the borate bridge in seamanite. The O(1)–O(4) distance is 2·494 (4) Å.

The adjacent-face-sharing triplets are linked together by further face-sharing to give infinite chains of face-shared iron-containing octahedra, the net direction of which is parallel to *c*. Parts of two such chains are shown in Fig. 3, which is a view of the structure perpendicular to the *bc* plane. One chain, partially obscured, is behind and below the other and is related to it by the *C*-centering translation. The adjacent-face-sharing triplets occur at each bend in the chain; the Fe(1) octahedra are thus located at each corner. The bridging phosphates are also shown.

The linear segments of the chain are composed of linear face-sharing triplets of the type which occur as trimers in several basic iron phosphates, such as dufrenite, rockbridgeite, and barbosalite (Moore, 1970). There are two such crystallographically different (though topologically identical) linear triplets in $Fe_2(PO_4)Cl$. The triplet which appears horizontal in Fig. 3 is centered at an Fe(2) on a twofold axis and lies approximately parallel to *a*. The other triplet appears vertical in the figure and is centered at Fe(3)

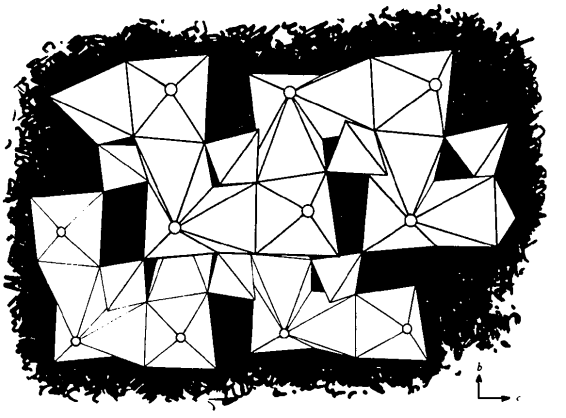

Fig. 3. Polyhedral representation of the $Fe_2(PO_4)Cl$ structure perpendicular to the *bc* plane. Cl atoms are represented by circles. See text for discussion.

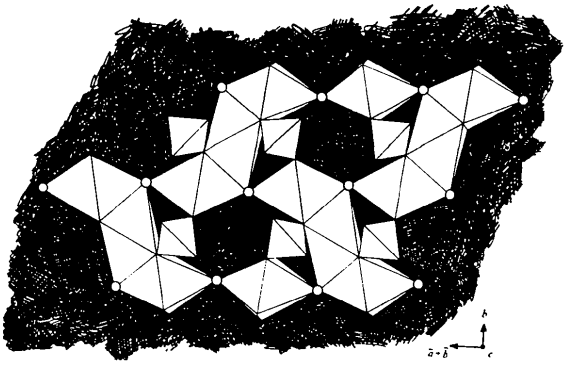

Fig. 4. Polyhedral representation of the $Fe_2(PO_4)Cl$ structure perpendicular to that of Fig. 3, *i.e.* in the [001] direction. Cl atoms are represented by circles. Each Fe(1)–Fe(3)–Fe(1) triplet shown belongs to a different chain of face-sharing octahedra.

on an inversion center. It forms an acute angle ($\sim 70°$) with the first triplet and is tilted approximately 38° with respect to *b*.

Adjacent chains of face-sharing octahedra are linked directly only by corner-sharing through the Cl atoms and indirectly through corner-sharing with phosphate tetrahedra. Both types of linkage can be seen in Fig. 4, which is a view of the structure perpendicular to that of Fig. 3, *i.e.* in the [001] direction. Only the Fe(1)–Fe(3)–Fe(1) triplets of different chains are shown.

A face-sharing chain of iron-containing octahedra has been reported in the synthetic 'iron lazulite' $Fe_{3\cdot6}(PO_4)_2(OH)_2$ (Katz & Lipscomb, 1951), in which the iron sites are '7/8 occupied' giving the ionic formula $Fe^{2+}_{2\cdot5}Fe^{3+}_{1\cdot0}(PO_4)_2(OH)_2$. Lindberg & Christ (1959) pointed out the structural relationship between this synthetic phase and the barbosalite minerals. Since Moore (1970) suggested the probable necessity of such a defect structure for face-sharing *chains* of octahedra in oxy–hydroxyl structures, we allowed the occupancy factors for the Fe and Cl sites to vary in an anisotropic refinement. No deficiency in any site was found.

The room-temperature Mössbauer-effect spectrum of $Fe_2(PO_4)Cl$ gave a doublet (obviously the result of a close overlap of three nearly equivalent doublets) with isomer shift 1·400 (8) mm s^{-1} (relative to sodium nitroprusside) and a quadrupole splitting of 2·035 (4) mm s^{-1}, characteristic of high-spin divalent Fe. No evidence for trivalent Fe was found. Magnetic-susceptibility measurements taken over the range of 9–78 K indicated antiferromagnetic behavior with $\theta = -29(2)$ K and a Néel temperature of less than 9 K. The magnetic moment per Fe atom derived from data in the paramagnetic region was 4·83 B.M., also in good agreement with the moment expected for divalent Fe.

Both the magnetic data and the iron–iron distances indicate a lack of Fe–Fe electronic interaction. The shortest Fe–Fe distances are Fe(1)–Fe(2) 3·082 (1), Fe(1)–Fe(3) 3·044 (1), and Fe(2)–Fe(3) 3·499 (1) Å.

The structure of $Fe_2(PO_4)Cl$, surprisingly, is unrelated to that of the isostructural compounds $Mn_2(PO_4)Cl$ (Rea & Kostiner, 1972*a*) and $Mg_2(PO_4)Cl$ (Rea & Kostiner, 1972*b*).

We are indebted to G. L. Shoemaker for preparing the polyhedral drawings. The magnetic data were recorded by A. H. Menotti and R. Paolino. This work was supported by the University of Connecticut Research Foundation and by the National Science Foundation (grant No. GH-42433). Computations were carried out at the University of Connecticut Computer Center.

References

BUSING, W. R., MARTIN, K. O. & LEVY, H. A. (1962). *ORFLS*. Oak Ridge National Laboratory Report ORNL-TM-305.

BUSING, W. R., MARTIN, K. O. & LEVY, H. A. (1964). *ORFFE*. Oak Ridge National Laboratory Report ORNL-TM-306.

GERMAIN, G., MAIN, P. & WOOLFSON, M. M. (1971). *Acta Cryst.* A**27**, 368–376.

International Tables for X-ray Crystallography (1974). Vol. IV. Birmingham: Kynoch Press.

KATZ, L. & LIPSCOMB, W. N. (1951). *Acta Cryst.* **4**, 345–348.

KOSTINER, E. & REA, J. R. (1974). *Inorg. Chem.* **13**, 2876–2880.

LINDBERG, M. L. & CHRIST, C. L. (1959). *Acta Cryst.* **12**, 695–697.

MOORE, P. B. (1970). *Amer. Min.* **55**, 135–169.

MOORE, P. B. (1971). *Amer. Min.* **56**, 1527–1538.

REA, J. R. & KOSTINER, E. (1972*a*). *Acta Cryst.* B**28**, 2505–2509.

REA, J. R. & KOSTINER, E. (1972*b*). *Acta Cryst.* B**28**, 3461–3464.

ZACHARIASEN, W. H. (1968). *Acta Cryst.* A**23**, 558–564.